Nuclear Science and Techniques **24** (2013) 050501

IMF production and symmetry energy in heavy ion collisions near Fermi energy

WADA Roy[1,*] HUANG Meirong[1] LIN Weiping[1,2] LIU Xingquan[1,2]
ZHAO Minghui[1,2] CHEN Zhiqiang[1]

[1]*Institute of Modern Physics, Chinese Academy of Science, Lanzhou 730000, China*

[2]*University of Chinese Academy of Sciences, Beijing 100049, China*

Abstract The symmetry energy at the time of the production of intermediate mass fragments (IMFs) is studied using experimentally observed IMF multiplicities combined with quantum statistical model calculations (QSM of Hahn and Stöcker). The ratios of difference in chemical potentials between neutrons and protons relative to the temperature, $(\mu_n-\mu_p)/T$, and the double ratio temperature, T, were extracted experimentally in the reactions of ^{64,70}Zn, ^{64}Ni+^{58,64}Ni, ^{112,124}Sn, ^{197}Au, ^{232}Th at 40A MeV. The extracted $(\mu_n-\mu_p)/T$ scales linearly with δ_{NN}, where δ_{NN} is the asymmetry parameter, $(N–Z)/A$, of the emitting source and $(\mu_n-\mu_p)/T=(11.1\pm1.4)\delta_{NN}-0.21$ was derived. The experimentally extracted $(\mu_n-\mu_p)/T$ and the double ratio temperatures are compared with those from the QSM calculations. The temperatures, T, and densities, ρ, extracted from the $(\mu_n-\mu_p)/T$ values agreed with those from the double ratio thermometer which used the yield ratios of d, t, h and α particles. However the two analyses of the differential chemical potential analysis and the initial temperature analysis end up almost identical relation between T and ρ. T=5.25±0.75 MeV is evaluated from the $(\mu_n-\mu_p)/T$ analysis, but no density determination was possible. From the extracted T value, the symmetry energy coefficient $E_{\rm sym}$=14.6±3.5 MeV is determined for the emitting source of T=5.25±0.75 MeV.

Key words Intermediate mass fragment production, Differential chemical potential, Double ratio temperature, Density, Symmetry energy and quantum statistical model

1 Introduction

The symmetry energy of nuclear matter is a fundamental ingredient in the investigation of nuclear and astrophysical phenomena[1,2]. In heavy ion reactions near the Fermi energy, different size isotopes, from Z=3 to those with Z up to Z of fission fragments, are copiously produced and the isotopic yields, which are a function of temperature and density at the time of the isotope formation, carry information on the symmetry energy of the emitting source. However the production mechanisms of these isotopes are not always completely understood. Global characteristic features of the experimental observables, such as multiplicities, mass or charge distributions and energy spectra or the mean energies of the fragments, have been well reproduced by both statistical multifragmentation models[3,4] and by dynamic transport models[5,6], though the two are based on quite different assumptions.

In order to further elucidate the reaction mechanisms and the characteristic nature of the emitting source, detailed experimental information, such as temperature and density of the emitting source, is indispensable. Temperature has been experimentally extracted mainly in two methods in this energy domain. One utilized the relative population of excited states of fragments[7-13]. The other method utilized the double yield ratios of isotopes[12-17]. Both results were

Supported by National Natural Science Foundation of China (NSFC) Projects (No.11075189), "100 Persons Project (Nos. 0910020BR0 and Y010110BR0)" and "ADS project 302" of the Chinese Academy of Sciences (No. Y103010ADS). Also supported by U.S. Department of Energy (Grant No. DE-FG03-93ER40773) and Robert A. Welch Foundation (Grant A0330).

* Corresponding author. *E-mail address:* wada@comp.tamu.edu

Received date: 2013-06-27

consistent near the Fermi energy. However when the incident energy increases, these two methods can give different results. In the study of Kr+Nb at 35–120*A* MeV by Xi *et al.*[13], the relative population temperature shows more or less a constant temperature of around 4 MeV, independent of the incident energies, whereas the double ratio temperatures, derived from He and Li isotopes, steadily increase from 4.7 to 9 MeV as the incident energy increases. This increase, however, is not observed for the double ratio temperature of Li and C isotopes, which shows a rather constant temperature of around 5 MeV. Similar results were reported in Au+Au reactions at 50–200*A* MeV[16,17]. From these observations, Trautmann *et al.*[17] concluded that two thermometers probe the temperature at different stages of the reaction.

In our recent works[18-21], the density of the emitting source was also extracted, together with the temperature, utilizing a coalescence model technique. The model was applied to the light charged particles (LPC's) from the reactions of ^{40}Ar+^{112,124}Sn and ^{64}Zn+^{112,124}Sn at 47*A* MeV[22-26]. A 4π detector, NIMROD, was used in the experiment[27]. The temperature of the emitting source was evaluated from the double yield ratios of $Y(d)/Y(t)$ and $Y(^3\mathrm{He})/Y(\alpha)$. The density was extracted, employing the thermal coalescence model of Mekjian[28]. The extracted temperature and the density show more or less a linear correlation, that is, as the temperature decreases from 11 MeV to 5 MeV, the density decreases from $0.2\rho_0$ to $0.03\rho_0$, where ρ_0 is the normal nuclear density.

The low density symmetry energy coefficients extracted were quite different from those extracted in previous works in a similar incident energy range, E_{sym}~15–20 MeV and ρ/ρ_0~0.3–0.6[29]. Therefore it is very interesting to extend the previous study to heavier isotopes. The IMF energy is significantly modified by the Coulomb repulsion and possible radial flow. The yield of IMF's is also modified by sequential secondary decay process as discussed in our recent works[30-32]. Therefore in order to study the density and symmetry energy coefficient for IMF emission, we derived, from the data, the ratio of the difference in chemical potential between neutrons and protons to the temperature, $(\mu_n-\mu_p)/T$, which is rather insensitive to the secondary cooling process. The differential chemical potential, $(\mu_n-\mu_p)$, is also closely related to the symmetry energy at the time of the fragment formation, i.e., $(\mu_n-\mu_p)=4E_{\mathrm{sym}}(\rho)\delta$ [33] as discussed below, where $\delta=(\rho_n-\rho_p)/(\rho_n+\rho_p)$. Using our data together with results of calculations employing the quantum statistical model (QSM) of Hahn and Stöcker[34], the correlations between density, temperature and symmetry energy coefficient are studied.

2 Experiment

The experiment was performed at the K-500 superconducting cyclotron facility at Texas A&M University. ^{64,70}Zn and ^{64}Ni beams were used to irradiate ^{58,64}Ni, ^{112,124}Sn, ^{197}Au and ^{232}Th targets at 40*A* MeV. A detailed description of the experimental setup and event classification has been given in Refs.[30,31]. Intermediate mass fragments (IMF's) were detected by a Si telescope placed at 20°, which consists of four quadrant Si detectors. Typically 6–8 isotopes for atomic numbers, *Z*, up to *Z*=18 were clearly identified with the energy threshold of 4–10*A* MeV, using the *ΔE–E* technique for any two consecutive detectors. The multiplicity of neutron and light charged particles (LCP) associated with each IMF were also measured by 16 DEMON detectors and 16 CsI(Tl) detectors around the target.

3 Results

3.1 Moving source fit

The yield of each isotope was evaluated, using a moving source fit, where a single intermediate velocity (*NN*) source with a smeared source velocity around half the beam velocity was used, coupled with the AMD simulations as a reference. A detailed procedure of the multiplicity extraction was given in Ref.[31]. For neutrons and LCPs, three moving source fit was applied, i.e., projectile-like source, *NN* source and target-like source. In the following analysis the multiplicity of the *NN* source is used for all particles as their multiplicity.

As direct outputs of the moving source fit, the source size $A_s=(N_s+Z_s)$ and asymmetry parameter, $\delta_{NN}=(N_s-Z_s)/A_s$, are evaluated from the extracted multiplicity as $N_s=\Sigma M_iN_i$ and $Z_s=\Sigma M_iZ_i$, where the

summation is taken over all measured particles, including neutrons, LCPs and IMF with Z up to 18. N_i and Z_i are neutron and proton number of the particle i. In Fig.1, the extracted A_s and δ_{NN} are plotted as a function of Z_{max}, the upper limit of the summation. A_s and δ_{NN} values at Z_{max}=2, for example, indicate the source size and asymmetry when only light particles are taken into account. The emitting source size of the *NN* component varies from 45 to 80 for the small (Ni) to the large mass (Th) target. This indicates that all *NN* source particles originate from a rather small source, about a half of the projectile for the Ni targets to a slightly large size of the projectile for the heavy targets. The observation of a rather small size of the emitting source is consistent with previous observations, which indicates that, as a function of temperature, experimental observables such as the isoscaling parameter, symmetry energy coefficient and pairing coefficient, reflect similar reaction mechanisms , even though the target sizes are quite different in the reactions studied[30-32].

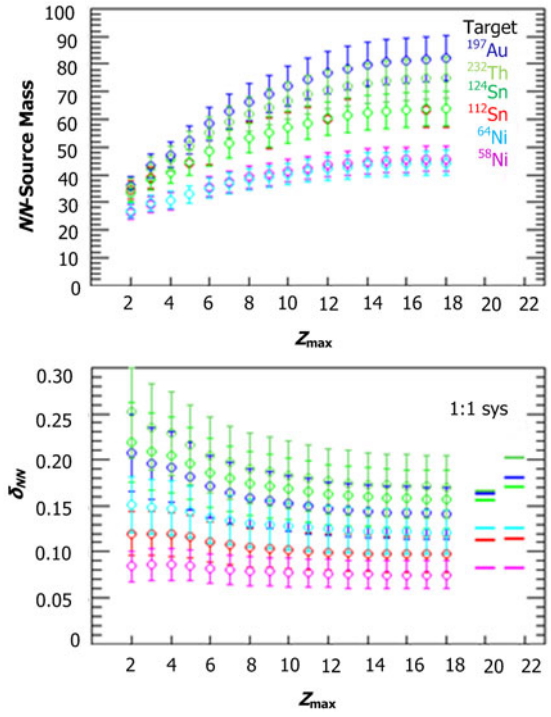

Fig.1 (Color online) Source size (top) and asymmetry δ_{NN} (bottom) of the *NN* source for reactions with the ^{64}Ni beam. Different targets are shown by different colors as indicated. Horizontal bars on the bottom right indicates the calculated δ_{NN} values from the source of 1 to 1 mixing of projectile and target nucleons and from the whole given reaction system, indicated by 1:1 and sys, respectively.

Within errors, the evaluated asymmetry parameter, δ_{NN}, is consistent with the values calculated assuming either from 1 to 1 mixing of the projectile and target nucleons or mixture of all nucleons. However the error bars, mainly originating from the moving source parameterization, are too large to determine the specific experimental asymmetry value for a given reaction system. Therefore in this work the calculated values of the 1 to 1 mixing source are used as δ_{NN} for the following analysis.

3.2 The ratio $(\mu_n-\mu_p)/T$

The ratio of the difference in nucleon chemical potential relative to the temperature, $(\mu_n-\mu_p)/T$, can be experimentally determined from the isotopic yield ratios, using the Modified Fisher Model[35-37]. In the Modified Fisher model, the fragment yield of A nucleons with $I=N-Z$, $Y(A, I)$, is given by

$$Y(A,I) = CA^{-\tau}\exp\{[(W(A,I)+\mu_n N+\mu_p Z)/T] + N\ln(N/A) + Z\ln(Z/A)\}, \quad (1)$$

where C is a constant. The $A^{-\tau}$ term originates from the entropy of the fragment and the last two terms are from the entropy contributions for the mixing of two substances in the Fisher Droplet Model[38]. $W(A,I)$ is the free energy of the cluster at temperature T. In our application $W(A,I)$ is given by the following generalized Weiszäcker-Beth semi-classical mass formula[39,40].

When the yield ratio of two isotopes between $I=I$ and $I=I+2$ with same A is taken, $R(I+2,I,A)=Y(A,I+2)/Y(A,I)$ is given by

$$R(I+2,I,A) = \exp\{[W(I+2,A)-W(I,A) + (\mu_n-\mu_p)]/T + S_{\mathrm{mix}}(I+2,A) - S_{\mathrm{mix}}(I,A)\}, \quad (2)$$

where $S_{\mathrm{mix}}(I,A)=N\ln(N/A)+Z\ln(Z/A)$. From these relations, one can get

$$R(I+2,I,A) = \exp\{[\mu_n-\mu_p+2a_c(Z-1)/A^{1/3} - 4a_{\mathrm{sym}}(I+1)/A-\delta(N+1,Z-1) - \delta(N,Z)]/T+\Delta(I+2,I,A)\}, \quad (3)$$

where $\Delta(I+IA)=S_{\mathrm{mix}}(I+A)S_{\mathrm{mix}}(IA)$, a_c and a_{sym} are the Coulomb and symmetry coefficient in $W(I,A)$ and $\delta(N,Z)$ represent the pairing term.

When we focus on the yields of isobars with I=–1 and 1, one can get

$$\ln\left[R(1,-1,A)\right]=\left[\left(\mu_n-\mu_p\right)+2a_c\left(Z-1\right)/A^{1/3}\right]/T. \quad (4)$$

This equation was initially applied to the ^{64}Zn+^{112}Sn reaction. ln[R(1,–1,A)] values were calculated from the multiplicities of isotopes in the atomic number range of 3≤Z≤18. $(\mu_n-\mu_p)/T$=0.71 and a_c/T=0.35 were extracted[31]. Assuming the same temperature and density at the time of the fragment formation for different reaction systems, which results in the same Coulomb energy contribution in Eq.(4), $(\mu_n-\mu_p)/T$ is evaluated as:

$$(\mu_n-\mu_p)/T=\left\langle\ln\left[R(1,-1,A)\right]\right\rangle-\left\langle 2a_c(Z-1)/A^{1/3}/T\right\rangle. \quad (5)$$

Here $\left\langle\ln\left[R(1,-1,A)\right]\right\rangle$ and $\left\langle 2a_c(Z-1)/A^{1/3}/T\right\rangle$ are the averaged experimental value over a certain range of Z of isotopes. Isotopes with $3\le Z\le 12$ are used, in order to minimize the errors between the reaction systems, since the statistics of higher Z isotopes becomes low for some of the reaction systems in the experiment. The resultant $(\mu_n-\mu_p)/T$ is shown in Fig.2 as a function of the asymmetric parameter $\delta_{NN}=(N-Z)/A$ of the emitting source. The values are well scaled by δ_{NN}. $(\mu_n-\mu_p)/T=11.1\delta_{NN}\pm 0.21$ is obtained as shown in the figure.

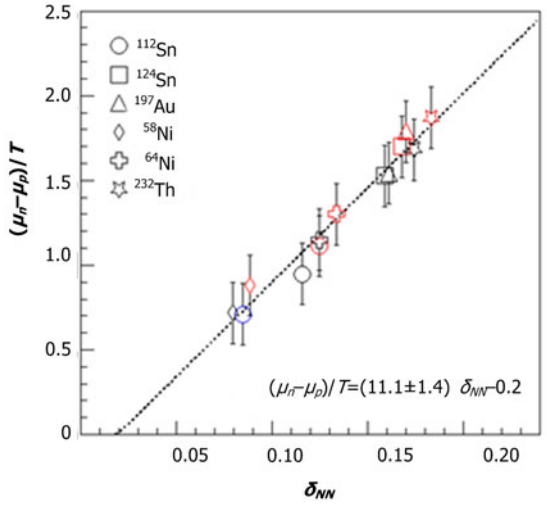

Fig.2 (Color online) $(\mu_n-\mu_p)/T$ vs δ_{NN} from all 13 reactions. Red, black and blue represent for ^{64}Ni, ^{70}Zn and ^{64}Zn beams, respectively. Results for different targets are also indicated by different symbols as shown. Data are fit by a linear function and the parameters are shown in the figure.

3.3 Temperature

In order to determine the temperature at the time of the fragment formation, the double isotope ratio thermometer between different IMF isotopes was used. The double isotope ratio temperature is generally given by

$$T=B/\ln(aR), \quad (6)$$

where R is the double yield ratio of four isotopes, B is a binding energy parameter and a relates to their spins[20]. There are many choices of the double ratio thermometers. Here we examined the following thermometers[25],

$$T_{pdh\alpha}=\frac{13.3\ \text{MeV}}{\ln\left\{5.5Y(p)/Y(d)/Y(h)/Y(\alpha)\right\}}, \quad (7)$$

$$T_{dth\alpha}=\frac{14.3\ \text{MeV}}{\ln\left\{1.6Y(d)/Y(t)/Y(h)/Y(\alpha)\right\}}, \quad (8)$$

$$T_{\text{LiBe}t\alpha}=\frac{14.2\ \text{MeV}}{\ln\left\{2.2Y(^6\text{Li})/Y(^7\text{Be})/Y(t)/Y(\alpha)\right\}}, \quad (9)$$

$$T_{\text{LiLi}h\alpha}=\frac{13.3\ \text{MeV}}{\ln\left\{2.2Y(^6\text{Li})/Y(^7\text{Li})/Y(h)/Y(\alpha)\right\}}, \quad (10)$$

$$T_{\text{BeLi}}=\frac{11.3\ \text{MeV}}{\ln\left\{1.8Y(^9\text{Be})/Y(^8\text{Li})/Y(^7\text{Be})/Y(^9\text{Li})\right\}}, \quad (11)$$

$$T_{CC}=\frac{13.8\ \text{MeV}}{\ln\left\{7.9Y(^{12}\text{C})/Y(^{13}\text{C})/Y(^{11}\text{C})/Y(^{12}\text{C})\right\}}. \quad (12)$$

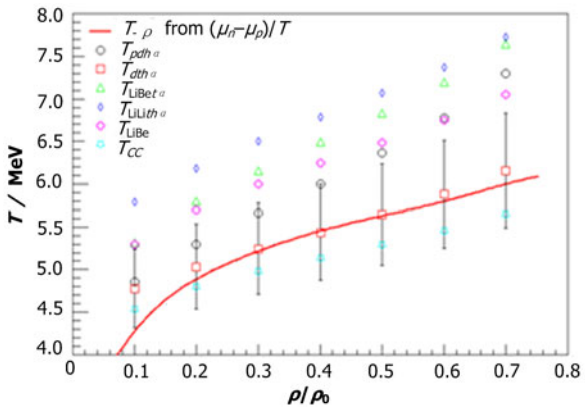

Fig.3 (Color online) Primary temperature vs emitting source density. Symbols are from the double ratio temperatures and typical errors are given only for the results from $T_{dth\alpha}$. The others have a similar errors in each point. Solid line is the result from $(\mu_n-\mu_p)/T$ fit.

The calculated values from the different thermometers represent the temperatures of the final products, which may be significantly modified by the secondary

statistical decay in the cooling process. The secondary decay effects are carefully examined, using the QSM calculation as described in Ref.[25]. The resultant primary temperatures extracted are fitted by a polynomial function of the secondary temperature for a given density. In Fig.3 the calculated primary temperature for these different thermometers are shown as a function of the density of the emitting source. The secondary temperatures used are those averaged over all 13 reactions. For all cases the primary temperature increases when the source density increases.

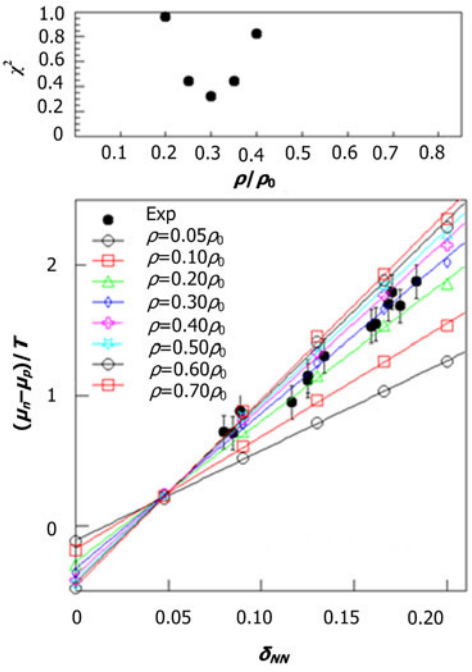

Fig.4 (Color online) (bottom) Experimental and calculated $(\mu_n-\mu_p)/T$ values as a function of δ_{NN}. T=5.2 MeV is used in the figure. The different symbols represent the values for different given densities as indicated. (top) Chi-square values as a function of the density.

For a given temperature and density in Fig.3, the differential chemical potential, $(\mu_n-\mu_p)/T$, is calculated, using QSM and compared with the experimental values in Fig.2. An example is shown in Fig.4 for the case T=5.2 MeV. For a given density and δ_{NN}, the differential chemical potential, $(\mu_n-\mu_p)/T$, is calculated. The density is varied from $0.05\rho_0$ to $0.7\rho_0$ in this case. For a given density, $(\mu_n-\mu_p)/T$ increases linearly as δ_{NN} increases, as shown in the bottom of Fig.4. From the chi-square fit, $\rho=0.3\rho_0$ is extracted for the case. T<4.5 MeV and T>6.0 MeV, no solution is found to get the minimum chi-square value below 0.4. T and ρ/ρ_0 values at the minimum chi square are plotted by a solid curve in Fig.3. From the results of $(\mu_n-\mu_p)/T$ analysis, the possible temperature range of 4.5≤T≤6.0 MeV was evaluated, but no specific density range was able to be determined in these methods.

3.4 Symmetry energy

The energy per nucleon of an asymmetric nuclear matter is approximately given by

$$E(\rho,\delta)=E(\rho,0)+E_{\rm sym}(\rho)\delta^2. \quad (13)$$

On the other hand the differential chemical potential is given by

$$(1/2)(\mu_n-\mu_p)=\partial E(\rho,\delta)/\partial\delta. \quad (14)$$

From these equations, one can get $(\mu_n-\mu_p)=4E_{\rm sym}(\rho)\delta$ [33]. In Fig.2, the experimental data are fit by a linear function and $(\mu_n-\mu_p)/T=(11.1\pm1.4)\delta-0.2$ is obtained. Using $(\mu_n-\mu_p)=4E_{\rm sym}(\rho)\delta$ from Eq.(14) and 4.5≤T≤6.5 MeV, $E_{\rm sym}$ coefficient is evaluated as $E_{\rm sym}$=14.6±3.5 MeV.

4 Conclusion

The differential chemical potential relative to the temperature, $(\mu_n-\mu_p)/T$ and the initial temperature T are studied, using the QSM calculation. The experimentally extracted $(\mu_n-\mu_p)/T$ values from the reactions studied show a linear function of δ_{NN} and $(\mu_n-\mu_p)/T=(11.1\pm1.4)\delta_{NN}-0.2$ was extracted. By comparison to the results of QSM calculations, possible T–ρ values for the emitting source were extracted. The extracted values are consistent with those of the initial temperature from the double isotope temperature of d, t, h and α isotopes. The extracted temperature range is 4.5≤T≤6.0 MeV. The symmetry energy coefficient $E_{\rm sym}$ is also evaluated from the slope value of 11.1±1.4 in the extracted experimental relation $(\mu_n-\mu_p)/T=(11.1\pm1.4)\delta_{NN}-0.2$ and in the above temperature range. $E_{\rm sym}$=14.6±3.5 MeV was obtained.

Acknowledgments

We thank all our colleges who participated in the experiment and the analysis; Wang J. from IMP, Rodrigues M. R. D., Hagel K., Barbui M., Bonasera A.,

Bottosso C., Natowitz J. B., Qin L. and Schmidt K. J. from TAMU, Keutgen T. from FNRS and IPN, Université Catholique de Louvain, Belgium and Kowalski S. from Institute of Physics, Silesia University, Poland. We also thank the staff of the Texas A&M Cyclotron facility for their support during the experiment. The author also thanks the program of Visiting Professorship for Senior International Scientists sponsored and funded by the Chinese Academy of Sciences.

References

1 Li B A, Chen L W, Ko C M. Phys Rep, 2008, **464:** 113–281.
2 Lattimer J M and Prakash M. Phys Rep, 2007, **442:** 109–165
3 Gross D H E. Rep Prog Phys, 1990, **53:** 605–658.
4 Bondorf J P, Botvina A S, IIjinov A S, *et al.* Phys Rep, 1995**, 257:** 133–221.
5 Aichelin J. Phys Rep, 1991, **202:** 233–360.
6 Ono A and Horiuchi H. Prog Part Nucl Phys, 2004, **53:** 501–581.
7 Nayak T K, Murakami T, Lynch W G, *et al.* Phys Rev C 1992, **45:** 132–161.
8 Kunde G J, Pochodzalla J, Aichelin J, *et al.* Phys Lett B, 1991, **272:** 202–206.
9 ChitwoodC B, GelbkeC K, Pochodzalla J, *et al.* Phys Lett B, 1986, **172:** 27–31.
10 Xi H, Zhan W L, Zhu Y T, *et al.* Nucl Phys A, 1993, **552:** 281–292.
11 Huang M J, Xi H, Lynch W G, *et al*. Phys Rev Lett, 1997**, 78:** 1648–1651.
12 Tsang M B, Zhu F, Lynch W G, *et al*. Phys Rev C, 1996, **53:** R1057–R1060.
13 Xi H F, Kunde G J, Bjarki O, *et al.* Phys Rev C, 1998**, 58:** R2636–R2639.
14 Albergo S, Costa S, Costanzo E, *et al.* Nuovo Cimento A, 1985, **89:** 1–28.
15 PochodzallaJ, Möhlenkamp T, Rubehn T, *et al.* Phys Rev Lett, 1995, **75:** 1040–1043.
16 Serfling V, Schwarz C, Bassini R, *et al*. Phys Rev Lett, 1998, **80:** 3928–3931.
17 Trautmann W, Bassini R, Begemann-Blaich M, *et al*. Phys Rev C, 2007, **76:** 064606.
18 Natowitz J B, Röpke G, Typel S, *et al*. Phys Rev Lett, 2010, **104:** 202501.
19 Hagel K, Wada R, Qin L, *et al.* Phys Rev Lett, 2012, **108:** 062702.
20 Qin L, Hagel K, Wada R, *et al*. Phys Rev Lett, 2012, **108:** 172701.
21 Wada R, Hagel K, Qin L, *et a*l. Phys Rev C, 2012, **85:** 064618.
22 HagelK, Wada R, Cibor J, *et al*. Phys Rev C, 2000, **62:** 034607.
23 Wang J, Keutgen T, Wada R, *et al*. Phys Rev C, 2005, **71:** 054608.
24 Wang J, Wada R, Keutgen T, *et al*. Phys Rev C, 2005, **72:** 024603.
25 Wang J, Keutgen T, Wada R, *et al*. Phys Rev C, 2007, **75:** 014604.
26 Kowalski K, Natowitz J B, Shlomo S, *et al*. Phys Rev C, 2007, **75:** 014601.
27 Wuenschel S, Hagel K, Wada R, *et al*. Nucl Instrum Methods A, 2009, **604:** 578–583.
28 Mekjian A Z. Phys Rev C, 1978, **17:** 1051–1070; Phys Rev Lett, 1977, **38**, 640–643.
29 Shetty D V, Yennello S J, Souliotis G A. Phys Rev C, 2006, **76:** 024606.
30 Huang M, Chen Z, Kowalski S, *et al*. Phys Rev C, 2010, **81:** 044620.
31 Huang M, Wada R, Chen Z, *et al*. Phys Rev C, 2010, **82:** 054602.
32 Chen Z, Kowalski S, Huang M, *et al*. Phys Rev C, 2010, **81:** 064613.
33 Danielewicz P and Lee J. Nucl Phys A, 2009, **818:** 36–96.
34 Hahn D and Stöcker H. Nucl Phys A, 1988**, 476:** 718–772.
35 Minich R W, Agarwal S, Bujak A, *et al.* Phys Lett B, 1982, **118:** 458–460.
36 Hirsch A S, Bujak A, Finn J E, *et al.* Nucl Phys A, 1984, **418:** 267–287.
37 Bonasera A, Chen Z, Wada R, *et al.* Phys Rev Lett, 2008, **101:** 122702.
38 Fisher M E. Rep Prog Phys, 1967, **30:** 615–730.
39 Weizsäcker C F. Z Phys, 1935, **96:** 431–458.
40 Bethe H A and Bacher R F. Rev Mod Phys, 1936, **8:** 82–229.